Hydro-geochemical elucidation and its implications in the Wardha valley coalfields of central India

To cite this article: P S Ganvir and Rajeeva Guhey 2022 *IOP Conf. Ser.: Earth Environ. Sci.* **1032** 012015

Hydro-geochemical elucidation and its implications in the Wardha valley coalfields of central India

P S Ganvir[1*] and Rajeeva Guhey[2]
[1]Assistant Professor, Department of Geology, M. G. Arts, Science and Late N. P. Commerce College Armori, Maharashtra, India.

[2]Professor, Department of Geology, Govt. N. P. G. College of Science, Raipur, Chhattisgarh, India.

*priyadarshan.ganvir@gmail.com

Abstract. The performed endeavour is to elucidate the hydro-geochemistry of the groundwater in the Wardha valley coalfield of central India. Being a coalfield of well-appreciated coal exploiting region, many studies has also disclosed the prevailing contamination issues in the same. The study is motivated to understand the groundwater chemistry and its possible implications in contamination prevalence. The measured hydro-geochemical parameters from 45 groundwater samples have manifested the rock-water interaction as a controlling mechanism with the dominance of CaMgCl facies to the extent of 67 % to 81 % in pre- and post-monsoon respectively. The hydro-geochemical facies analysis specified the ascendency of strong acid (SO_4^{2-}-Cl^-- NO_3^-) over weak acids (HCO_3^-). Such domination not only lowers the pH of the groundwater but also provide an encouraging hydro-geochemical situation for contaminations. To mitigate the contaminations like of heavy metals in and around coalfields, the pre-deliberations of such hydro-geochemical studies should be much anticipated and the present study is in agreement to it.

1. Introduction

The key role of the water for the existence of the life is indisputable and its sufficient quality supply must be accessible to all [1]. The groundwater quality is one of the furthermost vital concerns for human habitations and the standards are established accordingly by various agencies depending upon situatedness [2]. The usual chemical makeup of the groundwater is driven by the geochemistry of the solid portion of the earth and the hydrochemistry of the hydrosphere [3]. In contemporary period the human interference has affected many groundwater regimes; especially in and around coalfields, where the groundwater quality and quantity alters simultaneously. The quality of groundwater has always been in limelight around the coalfields [4]. Numerous endeavours have ensured that the contaminants including heavy metals from the coal mines are potential to get released into the adjacent environment by processes like leaching [5]. Such contaminants may affect the groundwater regime for prolong period of time; say for example the heavy metals are stubborn pollutants in the groundwater and cannot be mitigated with ease. Though the pollutants like trace metals are largely immobile, their mobility under definite chemical setup exceeds the conventional rates and became a menace [6].

The endeavoured study in the present article deals with the elucidations of the hydro-geochemistry of the groundwater to comprehend the chemical setup augmenting the mobility of the contaminants like trace metals in the groundwater regime of the Wardha Valley coalfields. The interpretations made will not only descript the hydro-geochemistry but will also disclose the factors amplifying the long known groundwater contamination issues of the study area.

1.1. Study Area and Geology

The study area of 894.35 km^2 can be traced in the two district of Maharashtra viz., Chandrapur and Yavatmal, bounded within the latitude 19^0 50' 00" to 20^0 10' 00'' N and longitude 78^0 55' 00" to 79^0 25' 00" E and is traceable on toposheet no. 55L/16, 55 P/4, 55 P/8, 56 I/13, 56 M/1 and 56 M/5 (Figure 1). The study area is under uninterrupted quarrying for coal since many decades [7]. The landscape of the study area is somewhat uniform in elevation with very few raised topographies around mining region (especially anthropogenic) and along margin. The study area is a part of NW-SE trending Pranhita-Godavari sub-basin of the Gondwana basin located on the eastern limb of anticline plunging towards NNW [8]. The study area is fairly dominated by the rocks of Gondwana supergroup with Archean as the basement rocks (Table 1). The rocks of the Kamthi formation consisting ferruginous sandstone and variegated shale makes the top layer with the rocks of Talchir as the lowest layer sandwiching the grey-white sandstone of the Barakar formation. The only coal seam also referred as the Principal seam of the study area is hosted by the Barakar Formation [9]. Apart from the Gondwana rocks, few insignificant patches of neoproterozoic sediments are also observable in patches (Figure 1).

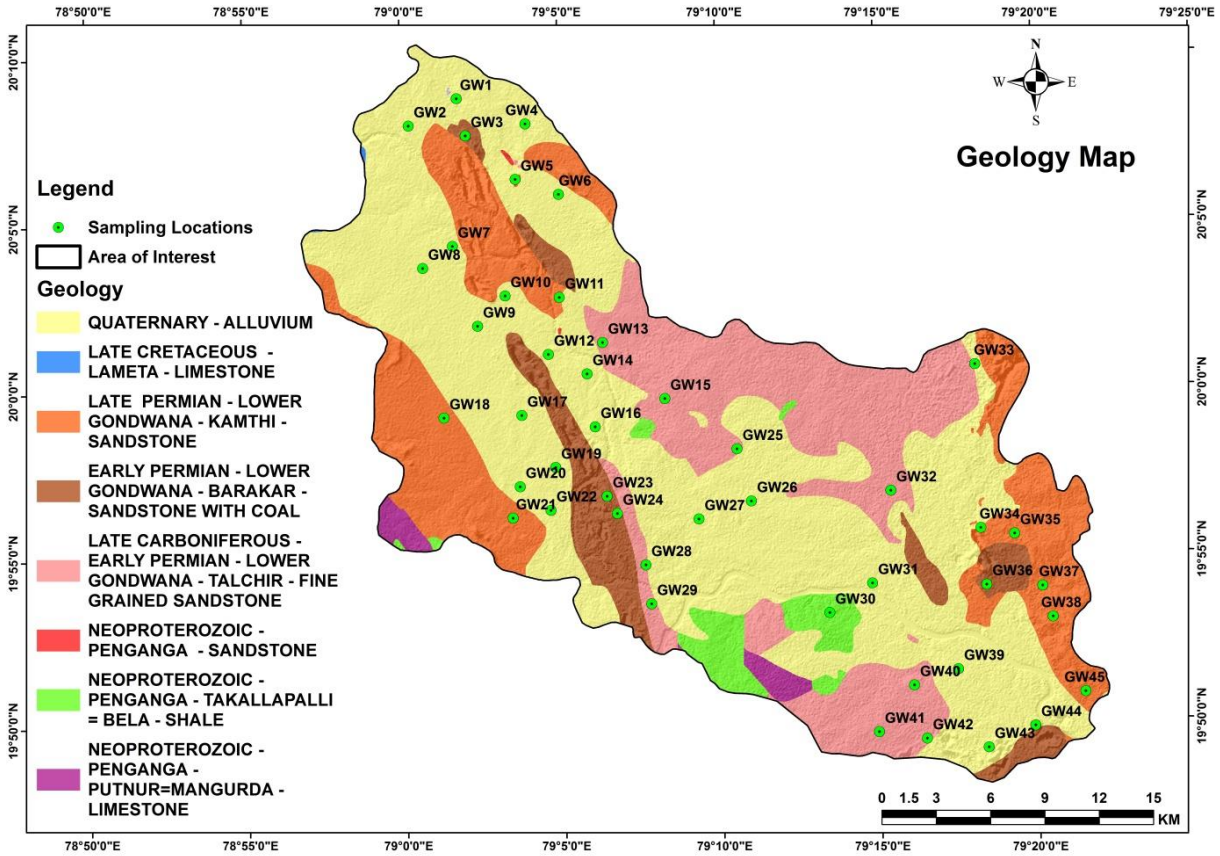

Figure 1. Geology map of the study area with groundwater sample locations [4].

Table 1. General Geological succession from Wardha Valley Coalfield, Maharashtra, [9].

Age	Group/Formation	Lithology
Recent	-	Alluvial gravel bed, black cotton soil
Eocene	Deccan Trap	Basalts
	----------Unconformity----------	
Cretaceous	Lameta Formation	Limestone, charts and silicified sandstone
	----------Unconformity----------	
Late Triassic	Maleri Formation (To South East)	Fine to med. Grained sandstone and red shale
Late Permian-Early Triassic	Kamthi Formation	Red, brown sandstone, reddish siltstone and variegated shale & sandstone
	----------Unconformity----------	
Early Permian	Barakar Formation	Light grey to white sandstone, shale & coal seam
Late Carboniferous-Early Permian	Talchir Formation	Tillites, turbidites, varves, needles shale & sandstone
	----------Unconformity----------	
Precambrian	Sullavai Sandstone	White and light brown quartzitic sandstone
	----------Overlap----------	
	Pakhal Limestone	Grey, bluish or pinkish limestone and chert
	----------Unconformity----------	
Archean		Quartzites, Granite gneisses, etc.

2. Methodology

In all, 45 groundwater samples were collected from pre-determined locations of the study area for both the seasons of 2020. The sampling locations were so fixed that to attain uniformity and appropriate representation to the manipulating factors like mining area, residential area and agricultural land. The samples were collected in agreement with the procedures suggested by APHA [10]. A pre-washed narrow mouth polyethylene container rinsed with the sample water was used to sample the groundwater. Physical suitability of the sampled groundwater was preferred to avoid any situation of filtration, which occasionally contributes contamination. To measure the fluctuating attributes like pH EC and TDS, spot analysis was performed by digital meter. The major ions in the sampled groundwater were analysed in the laboratory by the well-established procedures. The Ca^{2+} and Mg^{2+} are measured by respective titration methods; whereas, the Na^{+} and K^{+} are done by flame emission photometric method. Among anions, the HCO_3^{-} and Cl^{-} are measured by titrimetric method; while the SO_4^{2-} and NO_3^{-} are done by UV- spectrophotometric method. Once the results are deduced, the hydro-geochemistry was elucidated by the facies analysis through piper plots. The cause attributing the hydro-geochemistry was elucidated by Gibbs plots.

3. Result and Discussion

The assessment of the 45 groundwater samples collected from the study area has revealed the particulars of local hydro-geochemistry and has assisted in the corresponding elucidations. The data for the two succeeding seasons (pre-monsoon and post-monsoon) of 2020 was assessed attain the

aspired precision. The attempt to understand the hydro-geochemistry not only revealed the chemical nature of the groundwater but also reflected the effect of the host rocks over it.

3.1. Hydro-geochemical characterization of the groundwater

On equating to the post-monsoon samples, the pre-monsoons are certainly intense in concern to pH, TDS and anionic-cationic concentrations. The pH values of the samples are reasonably evident. The EC measurements has characterized that the 49 % of pre-monsoon observations are intense and lies in the range of 1500 μS/cm to 3000 μS/cm (not permissible); whereas, the post-monsoon observations are mild and only 09 % lies in the cited range (Table 2 and 3). The enhanced EC values can be attributed to the dissolved salts, which are quite obvious in pre-monsoons. As the EC somehow reflects the TDS; hence, the bulk of the observations range between the prescribed acceptable (500 mg/l) and permissible limit (2000 mg/l) (Table 2 and 3) [11].

The Ca^{2+} was observed to be the foremost cation among both the seasons (Figure 2) and its abundance in the observations is surpassing the recommended permissible limit of 200 mg/l in pre-monsoons by 07 % of total sample share; while, around 80 % of the them were between the recommended acceptable limit of 75 mg/l and permissible limit of 200 mg/l (Table 2a) [11]. In post-monsoon, the value of 80 % is reduced to 60 % (Table 3). The Mg^{2+} concentration in around 02 % observations of the pre-monsoons was found to be exceeding the recommended permissible limit of 100 mg/l. Whereas, in an average 87 % of the observations among them were between the recommended acceptable limit (30 mg/l) and permissible limit (100 mg/l) (Table 2) [11]. Similarly, around 30% of the observations were between the acceptable and permissible limit in the post-monsoon with no sample surpassing the 100 mg/l value (Table 3). The Na^{+} is the second abundant cation in the groundwater of the study area (Figure 2a and 3a). The average concentration of Na^{+} is 104.16 mg/l and 76.95 mg/l in pre- and post-monsoon respectively (Table 2 and 3). The concentrations of Na^{+} range widely within inter-seasons. The K^{+} existence can be accounted to the mineral like orthoclase, microcline and biotite from the lower Gondwana sediments. The concentrations of K^{+} were reasonably much lower than the Na^{+} (Table 2 and 3).

The HCO_3^{-} is the foremost factor which controls the alkalinity in the groundwater regime, especially when the pH is low. The observation reveals the HCO_3^{-} as the only anion accountable for the alkalinity in the groundwater of the study area with an average concentration of 295.57 mg/l and 217.86 mg/l in pre-and post-monsoon respectively (Table 2 and 3). The limestone beds of the Lameta formation in the study area can certainly be the source of the HCO_3^{-} in the groundwater. The average concentration of the Cl^{-} ranges from 122.1 mg/l to 74.2 mg/l for the pre-monsoon and post-monsoon seasons (Table 2 and 3). The concentration of the Cl^{-} was found to be well within the permissible limit of 1000 mg/l for all observations; whereas, around 4 % of the observations in the pre-monsoon were above the recommended acceptable limit of 250 mg/l [11]. The SO_4^{2-} is the principal anion in the observed groundwater samples especially in pre-monsoon season (Figure 2b). Around, 44 % and 04 % of the samples were above the permissible limit of 400 mg/l in pre- and post-monsoon respectively (Table 2 and 3). The NO_3^{-} is the least anionic contributor in the observed groundwater samples of both the seasons with mere an average concentration of 15.36 mg/l and 15.11 mg/l in pre- and post-monsoon respectively (Table 2 and 3).

Table 2: The results obtained for hydro-geochemical parameters from pre-monsoon groundwater samples.

Sample	Locations		pH	EC	TDS	Ca^{2+}	Mg^{2+}	Na^{+}	K^{+}	HCO_3^{-}	Cl^{-}	SO_4^{2-}	NO_3^{-}
GW1	20°08'46"N	79°01'48"E	6.9	1071	685	104	25	72	7.91	255	102	98	24.22
GW2	20°07'58"N	79°00'16"E	7.2	1240	794	141	29	62	5.77	215	132	162	3.12
GW3	20°07'39"N	79°02'04"E	6.5	1681	1076	141	64	82	9.12	291	81	410	12.08
GW4	20°07'59"N	79°03'58"E	6.7	1276	817	92	46	91	10.22	301	88	156	46.29
GW5	20°06'20"N	79°03'38"E	7.1	998	639	64	41	59	7.59	212	82	155	20.12
GW6	20°05'52"N	79°05'00"E	6.9	1177	753	102	39	64	5.33	229	159	115	22.89
GW7	20°04'21"N	79°01'37"E	6.4	1498	959	132	51	70	6.99	231	24	489	4.12
GW8	20°03'42"N	79°00'40"E	6.7	1079	691	98	42	51	6.42	270	110	102	37.09
GW9	20°01'57"N	79°02'23"E	6.1	2278	1458	141	88	160	21	278	290	444	7.33
GW10	20°02'51"N	79°03'16"E	6.2	1655	1059	132	81	70	10.22	217	33	562	5.22
GW11	20°02'47"N	79°04'59"E	6.1	1777	1137	163	66	81	7.71	266	31	555	7.88
GW12	20°01'05"N	79°04'37"E	5.9	2280	1459	151	86	173	16.07	322	217	428	5.44
GW13	20°01'25"N	79°06'20"E	6.6	1604	1027	91	66	119	10.1	329	101	271	33.77
GW14	20°00'29"N	79°05'50"E	5.9	2317	1481	194	102	98	8.23	298	189	504	21.62
GW15	19°59'43"N	79°08'17"E	6.1	1232	788	125	38	61	5.56	241	132	200	12.32
GW16	19°58'54"N	79°06'04"E	5.9	2602	1665	228	96	142	12.47	335	262	492	12.03
GW17	19°59'16"N	79°03'45"E	6	2174	1391	173	66	158	13.8	294	177	527	3.03
GW18	19°59'13"N	79°01'17"E	7.2	1343	860	127	41	77	8.32	274	121	150	12.42
GW19	19°57'42"N	79°04'48"E	5.9	2110	1350	170	66	142	13.07	351	139	490	6.02
GW20	19°57'08"N	79°03'40"E	6.4	1305	835	93	37	113	8.3	277	144	162	14.12
GW21	19°56'12"N	79°03'26"E	6.9	1176	753	93	42	70	5.12	341	76	122	8.6
GW22	19°56'25"N	79°04'38"E	5.7	2503	1602	222	91	131	16.41	369	199	561	11
GW23	19°56'49"N	79°06'25"E	5.9	2543	1628	234	79	142	14.23	402	182	524	24.55
GW24	19°56'18"N	79°06'44"E	6.1	2378	1522	179	88	141	12.04	323	211	490	9.09
GW25	19°58'11"N	79°10'33"E	6.4	1286	823	91	55	74	14.23	299	91	139	47.11
GW26	19°56'37"N	79°10'59"E	7.3	702	449	51	14	61	6.12	273	19	38	14.08
GW27	19°56'06"N	79°09'19"E	7.1	1136	727	77	34	101	7.67	351	77	133	8.22
GW28	19°54'45"N	79°07'37"E	6.2	2058	1317	172	55	152	15.89	388	162	389	5.43
GW29	19°53'35"N	79°07'47"E	6.3	1647	1054	129	78	73	9.02	276	41	421	10.9
GW30	19°53'15"N	79°13'25"E	6.8	1101	705	83	38	64	8	302	47	159	27.56
GW31	19°54'07"N	79°14'47"E	6.6	1095	701	62	48	81	6.06	298	48	142	15.02
GW32	19°56'53"N	79°15'24"E	7.2	831	532	69	27	52	6.77	326	31	55	4.12
GW33	20°00'38"N	79°18'07"E	6.3	1896	1213	106	60	171	21.88	211	73	561	18.9
GW34	19°55'44"N	79°18'14"E	5.9	2232	1428	136	77	196	20.2	280	235	471	13.08
GW35	19°55'33"N	79°19'18"E	6.6	822	526	54	22	72	4	304	42	66	4.2
GW36	19°54'02"N	79°18'24"E	5.9	1992	1275	117	91	143	12.7	223	212	414	31.88
GW37	19°53'59"N	79°20'10"E	6.3	1178	754	117	44	38	7.1	348	82	139	22
GW38	19°53'03"N	79°20'29"E	7.1	1133	725	104	42	53	4.89	342	67	106	9.7
GW39	19°51'31"N	79°17'28"E	6.2	1300	832	96	57	63	7.73	321	130	133	31.51
GW40	19°51'03"N	79°16'04"E	6.7	1376	881	73	51	113	12.76	389	90	157	8.7
GW41	19°49'40"N	79°14'56"E	7	976	625	82	30	61	4.78	293	72	90	5.53
GW42	19°49'27"N	79°16'27"E	5.8	1921	1229	131	52	169	9.77	219	178	434	21.12
GW43	19°49'10"N	79°18'24"E	5.8	2121	1357	127	76	183	18.67	221	154	591	8
GW44	19°49'48"N	79°19'53"E	5.7	2175	1392	139	84	162	14	342	170	436	8.66
GW45	19°50'48"N	79°21'29"E	6.1	2056	1316	139	61	176	22.07	374	190	374	11.13
Minimum			**5.7**	**702**	**449**	**51**	**14**	**38**	**4**	**211**	**19**	**38**	**3.03**
Maximum			**7.3**	**2602**	**1665**	**234**	**102**	**196**	**22.07**	**402**	**290**	**591**	**47.11**
Average			**6.41**	**1607.36**	**1028.7**	**123.22**	**57.02**	**104.16**	**10.58**	**295.57**	**122.1**	**302.6**	**15.36**

Values in mg/l

Table 3: The results obtained for hydro-geochemical parameters from post-monsoon groundwater samples.

Sample	Locations		pH	EC	TDS	Ca^{2+}	Mg^{2+}	Na^{+}	K^{+}	HCO_3^{-}	Cl^{-}	SO_4^{2-}	NO_3^{-}
GW1	20°08'46"N	79°01'48"E	7.1	973	623	63	44	59	4.23	213	87	126	12.11
GW2	20°07'58"N	79°00'16"E	7.4	932	596	87	18	72	5.12	222	110	98	8.23
GW3	20°07'39"N	79°02'04"E	6.9	1299	831	104	47	63	7.88	231	79	247	12.22
GW4	20°07'59"N	79°03'58"E	7	813	520	74	22	58	6.1	190	89	102	27.85
GW5	20°06'20"N	79°03'38"E	7.6	730	467	61	22	52	5.14	232	71	62	8.74
GW6	20°05'52"N	79°05'00"E	7.1	1062	680	97	32	68	5.32	231	134	99	13.1
GW7	20°04'21"N	79°01'37"E	6.8	1242	795	123	37	69	4.3	214	88	280	23.21
GW8	20°03'42"N	79°00'40"E	7.2	973	623	68	39	61	4.56	256	89	102	16.21
GW9	20°01'57"N	79°02'23"E	6.4	1263	808	107	47	77	9.07	242	70	251	8.22
GW10	20°02'51"N	79°03'16"E	6.6	1380	883	131	33	97	3.9	223	72	362	13.22
GW11	20°02'47"N	79°04'59"E	6.3	1512	968	125	52	93	8.81	218	105	352	22.76
GW12	20°01'05"N	79°04'37"E	6.2	1214	777	94	44	74	5.5	173	84	262	22.71
GW13	20°01'25"N	79°06'20"E	7.1	982	628	103	19	62	7.34	241	79	121	10
GW14	20°00'29"N	79°05'50"E	6.3	1195	765	82	38	101	7.67	188	66	284	31.69
GW15	19°59'43"N	79°08'17"E	6.9	992	635	73	32	51	10.24	219	89	64	51.67
GW16	19°58'54"N	79°06'04"E	6.1	1373	879	110	41	95	11.32	212	65	303	31.14
GW17	19°59'16"N	79°03'45"E	6.9	1178	754	116	38	47	12.67	213	45	271	21.01
GW18	19°59'13"N	79°01'17"E	7.8	702	449	64	19	41	5.83	271	53	27	6
GW19	19°57'42"N	79°04'48"E	6.2	1322	846	117	43	69	23.21	238	60	302	14
GW20	19°57'08"N	79°03'40"E	6.8	806	516	67	32	42	6.5	180	83	91	7.67
GW21	19°56'12"N	79°03'26"E	7.6	779	499	67	29	42	7.9	222	65	83	14.32
GW22	19°56'25"N	79°04'38"E	6.2	1304	835	104	53	74	3.75	249	77	287	8.75
GW23	19°56'49"N	79°06'25"E	6.3	1269	812	113	34	76	8	153	46	333	21.44
GW24	19°56'18"N	79°06'44"E	6.7	966	618	82	26	71	5.5	173	23	250	4.43
GW25	19°58'11"N	79°10'33"E	6.7	1020	653	63	24	111	8.02	220	124	102	33.6
GW26	19°56'37"N	79°10'59"E	7.5	883	565	51	29	75	7.3	295	60	73	7.38
GW27	19°56'06"N	79°09'19"E	7.1	826	529	85	21	43	4.1	240	69	92	11.28
GW28	19°54'45"N	79°07'37"E	6.5	1323	847	76	34	137	14.8	191	53	353	38.31
GW29	19°53'35"N	79°07'47"E	6.4	1379	883	88	46	109	10.04	183	44	391	27.84
GW30	19°53'15"N	79°13'25"E	7.1	871	557	58	26	69	5.87	271	59	82	8.66
GW31	19°54'07"N	79°14'47"E	7	799	511	59	25	73	8.34	283	71	42	12.7
GW32	19°56'53"N	79°15'24"E	7.4	660	422	43	12	71	8.33	284	31	41	4.55
GW33	20°00'38"N	79°18'07"E	6.4	1636	1047	97	61	132	14.99	236	97	414	18
GW34	19°55'44"N	79°18'14"E	6.2	1273	815	109	52	61	8.9	193	61	351	4.23
GW35	19°55'33"N	79°19'18"E	6.9	839	537	71	29	51	6.1	215	72	80	13.22
GW36	19°54'02"N	79°18'24"E	6.4	1230	787	84	31	121	7.17	232	31	295	23.54
GW37	19°53'59"N	79°20'10"E	6.9	832	532	74	21	53	7.67	181	112	77	6.2
GW38	19°53'03"N	79°20'29"E	7.4	727	465	46	21	71	3.12	185	83	51	7.16
GW39	19°51'31"N	79°17'28"E	7.1	821	525	56	22	72	6.16	193	111	51	7.91
GW40	19°51'03"N	79°16'04"E	6.9	833	533	52	18	81	9.14	194	104	71	9.5
GW41	19°49'40"N	79°14'56"E	7.1	831	532	88	30	54	4.3	170	88	79	6.43
GW42	19°49'27"N	79°16'27"E	6.1	1253	802	103	40	86	7.1	145	38	375	9.03
GW43	19°49'10"N	79°18'24"E	6.3	1699	1087	94	62	142	12.03	253	71	444	6.43
GW44	19°49'48"N	79°19'53"E	6	1591	1018	104	44	137	11	232	89	374	9
GW45	19°50'48"N	79°21'29"E	6.5	1278	818	91	38	100	13.7	204	42	348	4.54
	Minimum		**6**	**660**	**422**	**43**	**12**	**41**	**3.12**	**145**	**23**	**27**	**4.23**
	Maximum		**7.8**	**1699**	**1087**	**131**	**62**	**142**	**23.21**	**295**	**134**	**444**	**51.67**
	Average		**6.78**	**1085.88**	**694.93**	**84.97**	**33.93**	**76.95**	**7.95**	**217.86**	**74.2**	**198.77**	**15.11**

Values in mg/l

3.2. Interpretations

3.2.1. Percentage contribution. The percentage contributions of the cations and the anions for the pre-monsoon has disclosed the abundance in the order of $Ca^{2+}>Na^{+}>Mg^{2+}>K^{+}$ and $SO_4^{2-}>HCO_3^{-}>Cl^{-}>NO_3^{-}$ respectively (Figure 2). Whereas the order for post-monsoon is $Ca^{2+}>Na^{+}>Mg^{2+}>K^{+}$ and $HCO_3^{-}>SO_4^{2-}>Cl^{-}>NO_3^{-}$ (Figure 3).

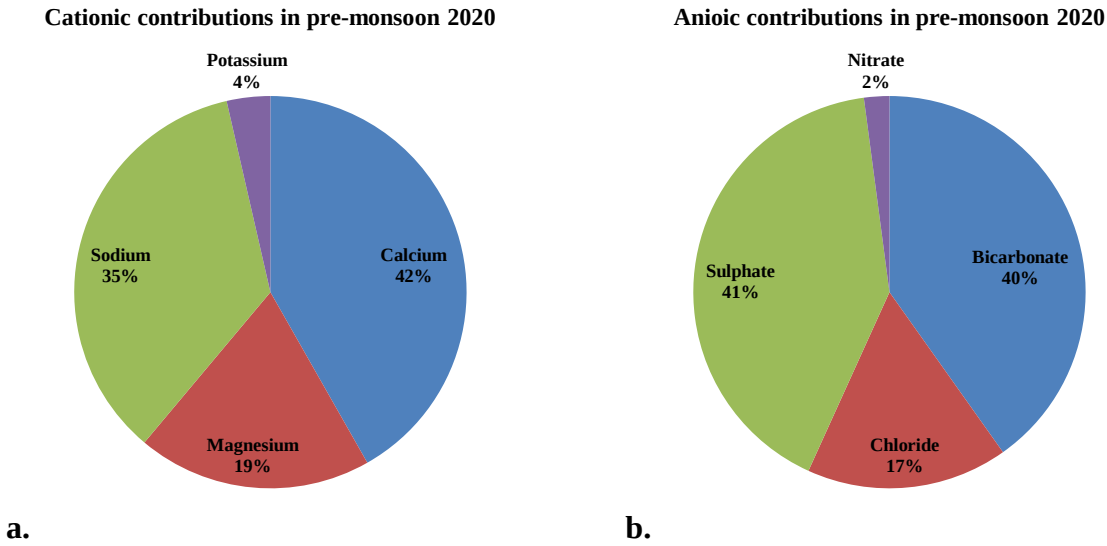

Figure 2: Percentage contribution of the ions in the pre-monsoon; **a.** Cations and **b.** Anions.

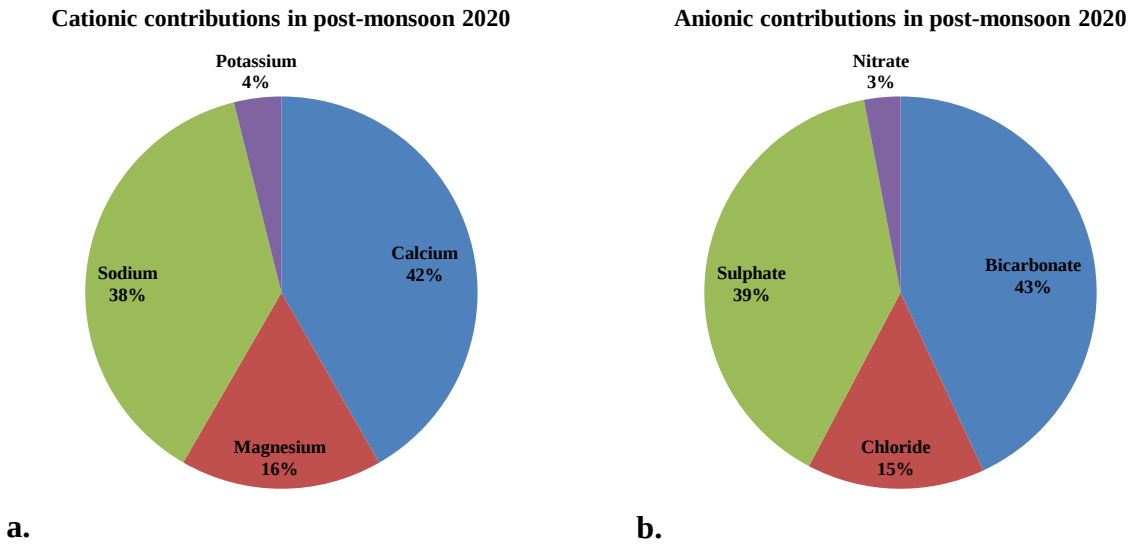

Figure 3: Percentage contribution of the ions in the post-monsoon; **a.** Cations and **b.** Anions.

3.2.2. Piper Plots. In the pre-monsoon season, around majority (67 %) of the groundwater samples point to the ascendancy of mixed CaMgCl type (zone 4); While, the rest samples are distributed between $CaHCO_3$ type (zone 1) and CaCl (zone 5) (Figure 4). The majority of the groundwater falls in Ca^{2+}-Mg^{2+}-Cl^{-}-SO_4^{2-} facies. In the cationic facies, about 93 % of the groundwater samples indicate no dominance. Whereas, in anionic facies, around 53 % of the samples are in the no dominance field and among the rest, 25 % are in the SO_4^{2-} type and 22 % are in the HCO_3^{-} type (Figure 4).

In post-monsoon, approximately majority (81 %) of the groundwater samples specifies the ascendency of mixed CaMgCl type (zone 4); while the rest are distributed among mixed $CaNaHCO_3$ type, $CaHCO_3$ type (zone 1) and CaCl (zone 5) (Figure 5). The majority of the groundwater falls in Ca^{2+}-Mg^{2+}-Cl^{-}-SO_4^{2-} facies in post-monsoon too. In the cationic facies, about 89 % of the groundwater samples are in no dominance. While in anionic facies, around 43 % of the samples are in the no dominance field, 41 % is in SO_4^{2-} type and rest 16 % is in HCO_3^{-} type.

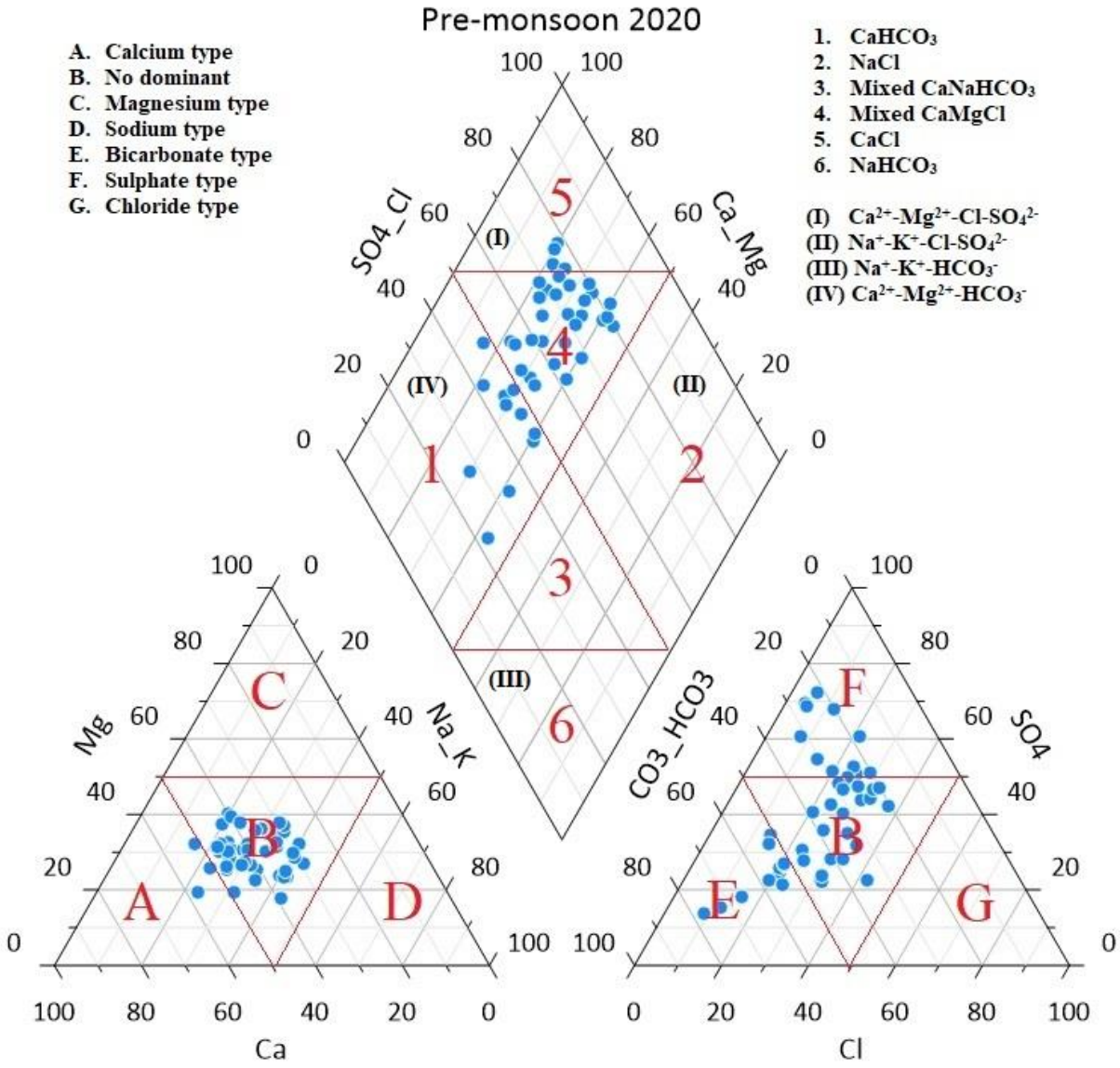

Figure 4: Piper diagram indicating the groundwater type in the pre-monsoon.

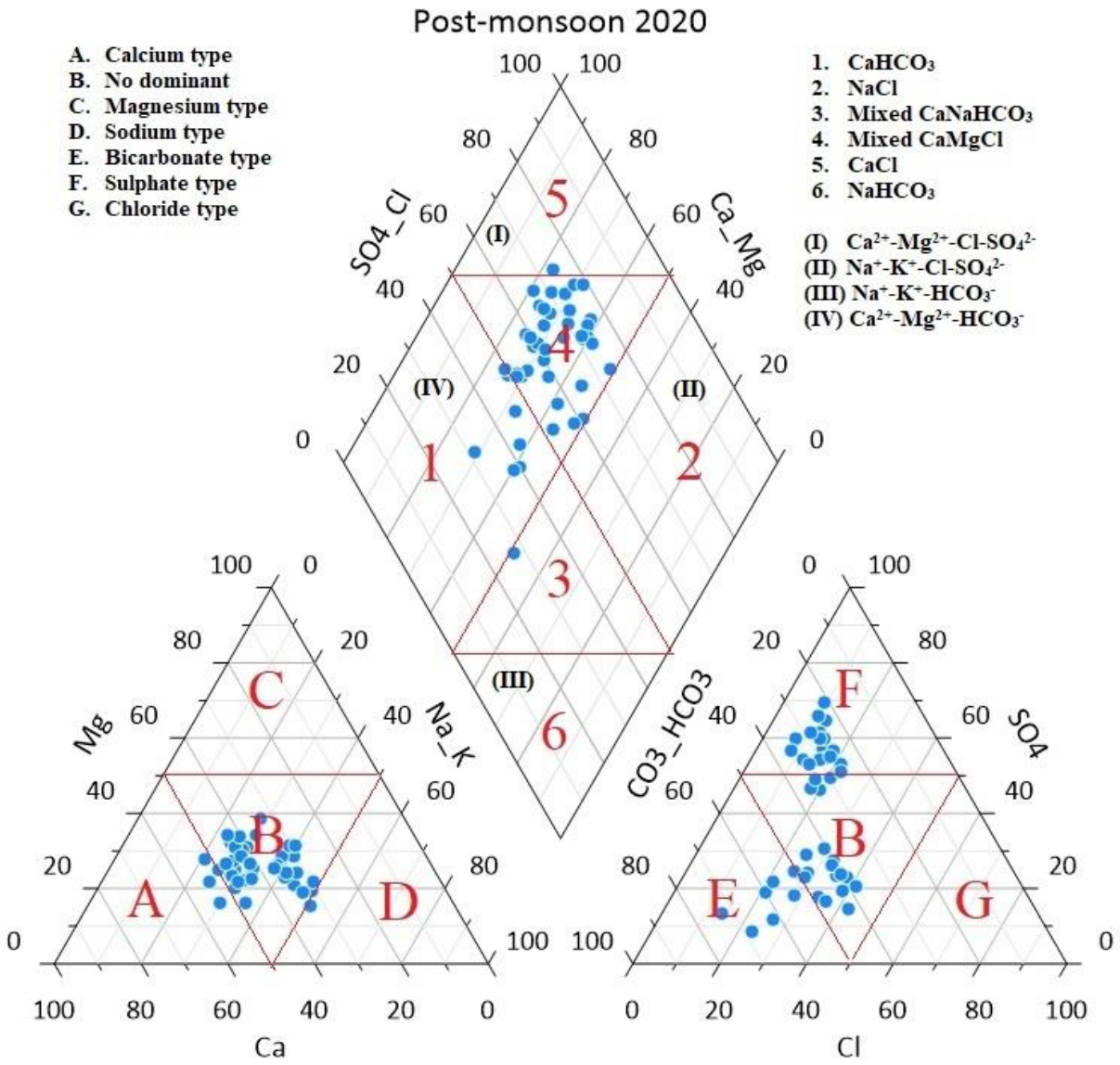

Figure 5: Piper diagram indicating the groundwater type in the post-monsoon.

3.2.3. Gibbs plot. The Gibbs plot indicates that the chemistry of the groundwater for the both the seasons. The groundwater chemistry is primarily governed by the rock-water interaction, with an insignificant influence of evaporation in pre-monsoon (Figure 6 and 7).

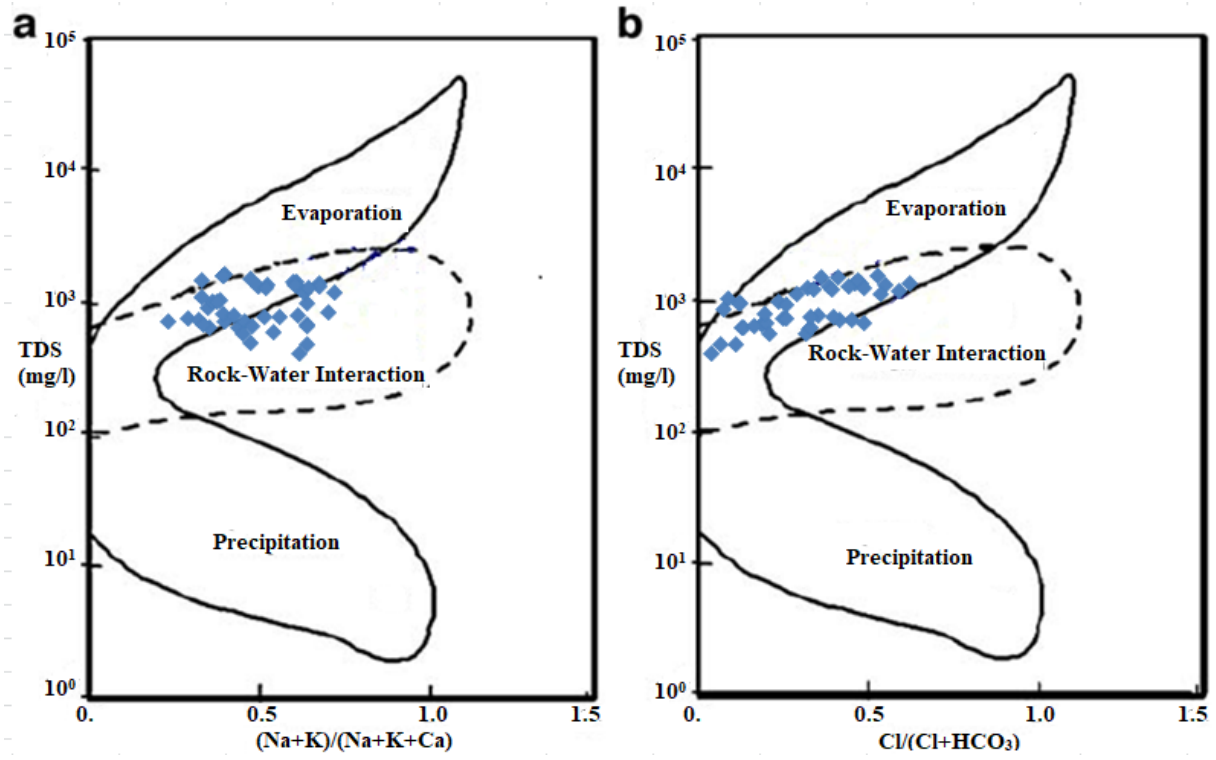

Figure 6: Gibbs diagram for the pre-monsoon; **a.** TDS vs. cations and **b.** TDS vs. anions.

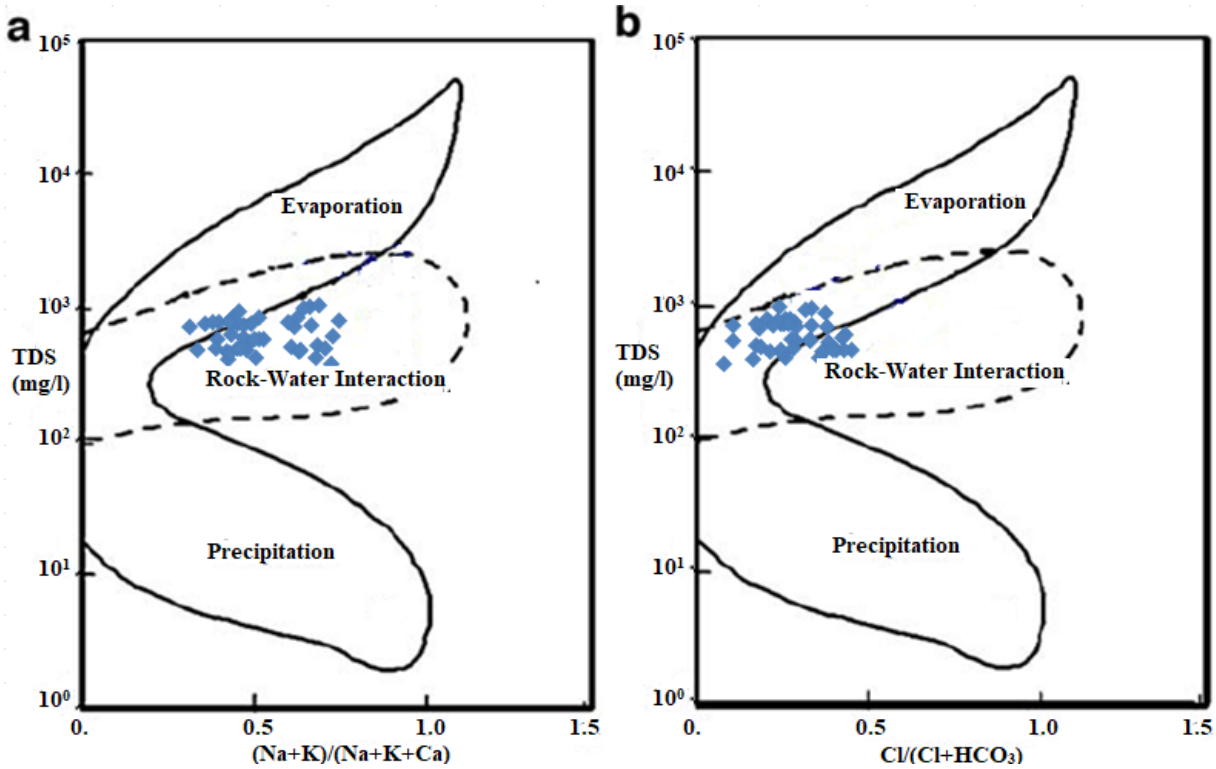

Figure 7: Gibbs diagram for the post-monsoon; **a.** TDS vs. cations and **b.** TDS vs. anions.

3.2.4. Implications of hydro-geochemical elucidations. The enhanced pH of the sampled groundwater can be attributed to the contributors like SO_4^{2-}, Cl^- and NO_3^- and its consequence in the hydro-geochemistry cannot be underrated. Water with low pH keeps potential of higher dissolving capacity as a result of which contaminants [12]. The acidic water ousted from coal mines are usually charged with the leachates from various sources like mine tailings, settling ponds, etc. resulting into severe pollutions [3]. As the groundwater from with lower pH is susceptible to to have high dissolvability, the higher TDS was quite expected. The enriched TDS can be attributed to the evaporative dominance conditions resulting into precipitation of the salts. The enriched concentration of the Ca^{2+} can be attributed to the plagioclase feldspar and the calcareous cementing material in the Barakar rocks of the Wardha valley coalfields is fairly attributable [13]. The Mg^{2+} concentration in the groundwater is certainly the result of water interaction with minerals like orthoclase, microcline and biotite of the lower Gondwana sediments. Similarly, the Na^+ can be guessed to be released from the minerals like feldspar, clay minerals, etc. of the lower Gondwana rocks of the study area. The limestone beds of the Lameta formation in the study area can certainly be the source of the enriched $HCO3^-$ concentration in the groundwater and is sole responsible for the alkalinity (predicted due to low pH). The dissolution of the NaCl from the rocks and soil is the prime process responsible for the higher Cl^- concentrations; whereas, the sewage effluents are also the considerable source for the same. The presence of the SO_4^{2-} in the groundwater regime lowers the pH through acid mine drainage [14]. The existence of the coal and sulphide minerals in the Barakar formation is accountable for the high concentration of the SO_4^{2-} in the groundwater [15]. Though the NO_3^- concentration is insignificant but could be responsible in lowering of pH of the groundwater. The most typical cause of in the groundwater is the decaying organic matter, sewage wastes and fertilizers.

The Gibbs plot has revealed the rock-water interaction as the controlling mechanism for groundwater chemistry. The same is also somewhat predictable by the ionic manifestation in the sampled groundwater. The hydro-geochemical facies analysis of the sampled groundwater has elucidated that the alkali earth (Ca + Mg) and the strong acids (SO_4^{2-}-Cl^-- NO_3^-) exceeds the alkalis (Na + K) and the weak acids (HCO_3^-) respectively. Such hydro-geochemical circumstances with dominance of strong acids are often favourable for the contaminations of heavy metals [16]. On correlating the sample locations and hydro-geochemical parameters, the intensities are found to be protruding around mining regions. Hence, observations are in somewhat agreement with the protruded contaminations in and around the mining locations are typical and go on decreasing away from the mining locations [17].

4. Conclusion

The major portion of the groundwater regime is dominated by the Ca^+-Mg^+ in cations and HCO_3^--SO_4^{2-} in anions. The hydro-geochemistry of the study area is majorly controlled by the rock-water interaction, where minerals from the host rocks are leached out. This process is augmented by the acidic nature of the groundwater (especially near mining regions) which can be attributed to the high SO_4^{2-} concentrations. The major groundwater is of CaMgCl type with no dominance of cations and distributed dominance of anions among no-dominance-HCO_3^--SO_4^{2-}. The hydro-geochemical facies analysis implies the ascendency of the strong acids (SO_4^{2-}-Cl^--NO_3^-) over weak acids (HCO_3^-). As a consequence of which, the groundwater conditions are quite favourable to the dissolution of contaminants like of heavy metals. The mitigation of such conditions is the most expected initiative to keep the groundwater potable in impending perspectives.

References

[1] WHO 1984 *Guidelines for drinking water qualities* (Washington DC: World Health Organisation) pp 35-43
[2] Ganvir P S and Guhey R 2020 Groundwater quality assessment with reference to some heavy metals toxicity and its probable remediation around Ballarpur area of Wardha valley coalfields, Maharashtra *IOP Conference Series: Earth and Environmental Science*, **597(1)** 012001
[3] Satapathy D R, Salve P R and Katpatal Y B 2009 Spatial Distribution of Metals in Ground/Surface Waters in the Chandrapur District (Central India) and heir Plausible Sources *Environmental Geology* **56** pp. 1323–52
[4] Ganvir P S and Guhey R 2021 Geochemical Studies of some Heavy Metals' Toxicity in Groundwater with their Plausible Sources around Gondwana Supergroup, Wardha valley Coalfields, Maharashtra *Journal Geological Society of India*, **97** pp. 1415-1421
[5] Filcheva E and Noustorova M 2000 Organic Accumulation and Microbial Action in Surface Coal-Mine Spoils, Pernik, Bulgaria *Ecological Engineering* **15** pp. 1–15
[6] Scokart P, Meeus-Verdinne K and DeBorger R 1983 Mobility of Heavy Metals in Polluted Soils near Zn Smelters *Water Air Soil Pollution* **20** pp. 451–63
[7] Singh R M and Chandra D 1983 Occurrence, Distribution and Probable Source of the Trace Elements in Ghugus Coals, Wardha Valley, District Chandrapur and Yeotmal, Maharashtra, India *International Journal Coal Geology* **24** pp. 371–81
[8] Sarate O P 2017 Petrography of Coal Seams from Wilson area, Chandrapur District, Maharashtra and their Depositional History *Geophytology* **47** pp. 193–201
[9] Raja Rao C S 1982 *Coal Resources of Tamil Nadu, Andhra Pradesh, Orissa and Maharashtra* (*Bulletin of the Geological Survey of India, coalfields of Maharashtra, Wardha Valley Coalfield* A vol 45) pp 85–87
[10] APHA 1998 *Standard Methods for the Examination of Water and Waste Water* 20th (Washington DC: Water Pollution Control Federation) pp 10 – 161
[11] BIS 2012 *Drinking Water - Specification (Second Revision) IS: 10500* (Bureau of Indian Standards) pp 2–3
[12] Zipper C, Skousen J and Jage C 2014 *Passive Treatment of Acid Mine Drainage* (Virginia: Virginia Polytechnic Institute and State University) pp 1–13
[13] Kale M G and Soman G R 2012 Petrography of Barakar Sediments from Ghugus Area, Pranhita-Godavari Basin, Maharashtra *Gondwana Geological Magazine* **27(1)** pp 67-78
[14] Singh G 1987 Mine Water Quality Deterioration due to Acid Mine Drainage *International Journal of Mine Water* **6** pp 49-61
[15] Karanth K R 1997 *Groundwater Assessment, Development and Management* Tata McGrraw Hill New Delhi p 720
[16] Ganvir P S and Guhey R 2020 Assessment of Some Heavy Metals Toxicity and Its Probable Remediation in Groundwater around Telwasa and Ghugus Area of Wardha Valley Coalfields, Maharashtra *Journal of Indian Association of Sedimentologists* **37(1)** pp 33-43
[17] Peplow D 1999 *Environmental Impacts of Mining in Eastern Washington* Centre for Water and Watershed Studies Fact Sheet, University of Washington, Seattle